Optimization of freeform spectacle lenses based on high-order aberrations

Keith Dillon[a] and Jeffrey Chomyn[a]

[a]Formulens, San Diego, USA

ABSTRACT

Spectacle lenses are an important application of freeform manufacturing, with complex designs such as progressive lenses requiring nontraditional and specialized surface shapes. Such lenses also pose special challenges for optical design, as the eye's gaze constantly changes relative to the lens. At the same time, many applications require sacrificing one region, such as the transition in a smooth bifocal, while achieving high quality in other regions. Common representations of freeform lens surfaces using polynomials or splines are poorly suited for such requirements. We describe an approach to optimize freeform spectacle lenses using a nonparametric representation of the surfaces at high resolution. Requirements for smoothness are quantified in terms of high-order aberrations. This allows us to describe spatial variations in the design while also incorporating a constraint for optical smoothness and manufacturability. We show how this can be formulated as a regularized optimization problem incorporating raytracing, which can be solved efficiently. The approach can be used to design various kinds of lenses including progressive, bifocal, and lenticular designs. The designs have been successfully manufactured on multiple different brands of freeform generators. Manufactured lenses are found to perform as designed, including without polishing when supported by the material and generator.

Keywords: Spectacle lens, high order aberrations, inverse design, lens optimization

1. INTRODUCTION

Spectacle lens design is a specialized niche of optics with unique challenges.[1] Eyes can have a wide range of refractive errors, with mainstream spectacles typically supporting a range of between +8 to -10 Diopters. Further, depending on the gaze direction, any point on the lens may be used for foveal vision, while the rest of the lens is used for peripheral vision (Fig. 1). Mitigating these challenges somewhat, the inherent chromatic and high-order aberrations of the eye provide a meaningful tolerance of about 0.25 Diopters. And while the eye's gaze may commonly vary up to 20 degrees from center or more, the field of view for any given gaze is limited; the rapid dropoff in cone density outside the fovea means we primarily need to consider only a small region of the lens at one time, when assessing vision quality at a particular gaze direction.

Freeform manufacturing for spectacles is also a specialized niche of optics. Most consumer lenses are made from some form of polymer or plastic, and either the front or back surface (or both) may be finished with a lathe. Typically, the front surface (away from the eye) is a molded spherocylindrical surface and the back is produced with the lathe. This is beneficial both in terms of cosmetic factors and cost. Modern lathes use a standard format to describe the spectacle surface, as a regular square grid with between 0.25 to 1.00 mm spacing. So the most general nonparametric approach to designing a lens surface for freeform manufacture is to directly optimize the values of this so-called height map.

Recent approaches to optimization for design have tended toward brute-force application of direct ideas such as to optimize the output of a ray-tracing simulator. Differentiable ray-tracing is a growing research area in other fields of optical design[2] which exploits modern scalable software and parallel computing techniques. However spectacle lens optimization remain very challenging when attempting to reconcile such approaches with a high-resolution representation and varying requirements across each point on the lens. This paper describes such a solution, where we optimize a nonparametric description of a surface given desired optical performance and with spatially-varying constraints on optical quality.

Further author information: (Send correspondence to K.D.)
K.D.: E-mail: kdillon@formulens.com, Telephone: 1 949 478 1736

2. METHODS

We start by considering a local approximation in the small-angle regime, which will form the inner step of an iterative lens optimization process. Note that most of the focal power of the spectacle-eye system will be provided by the eye itself (roughly 60 Diopters). And as noted previously, at any gaze direction we are primarily concerned with the limited field of view of foveal vision. So in a small-angle approximation, we can view the spectacle lens contribution as a wavefront phase adjustment provided by a small local region on the lens, as depicted in Fig. 1. The optical performance of the lens due (to each surface) is then the surface height scaled using the refractive

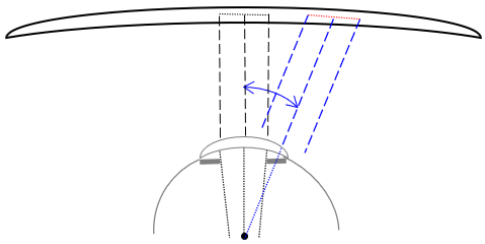

Figure 1. Small region of spectacle lens used for foveal (highest quality) vision which varies with the eye's gaze.

index. In terms of refractive errors, visual optical quality can be split roughly into low-order and high-order components of this wavefront. Low-order here incorporates defocus and astigmatism, which describe both the prescribed correction and the deviations from it. For our purposes, high-order describes optical aberrations such as coma and trefoil, and more generally any deviations from optical smoothness.

To understand the relationship to a conventional spherocylindrival surface, consider the two-dimensional Taylor expansion of the surface about the origin (for simplicity),

$$z(x,y) = z(0,0) + x\frac{\partial s}{\partial x} + \frac{1}{2}\left(x^2\frac{\partial^2 s}{\partial x^2} + xy\frac{\partial^2 s}{\partial x \partial y} + y^2\frac{\partial^2 s}{\partial y^2}\right) + \dots \tag{1}$$

We define the local curvature with the quadratic terms:

$$\alpha_{(2)}(x,y) = x^2\alpha_3 + xy\alpha_4 + y^2\alpha_5 = \begin{pmatrix} x \\ y \end{pmatrix}^T \begin{bmatrix} \alpha_3 & \frac{1}{2}\alpha_4 \\ \frac{1}{2}\alpha_4 & \alpha_5 \end{bmatrix} \begin{pmatrix} x \\ y \end{pmatrix} \tag{2}$$

The eigenvalues of the quadratic form are the principal curvatures

$$\lambda_\pm = \frac{1}{2}\left(\alpha_3 + \alpha_5\right) \pm \frac{1}{2}\sqrt{\left(\alpha_3 - \alpha_5\right)^2 + {\alpha_4}^2} \tag{3}$$

The mean and difference curvatures are

$$S = \lambda_+ + \lambda_- = \alpha_3 + \alpha_5 \tag{4}$$

$$C = \lambda_+ - \lambda_- = \sqrt{\left(\alpha_3 - s_5\right)^2 + {\alpha_4}^2} \tag{5}$$

S and C refer to "spherical" and "cylindrical" curvatures (note that constant offsets are not important here). These terms approximate the surface locally at each point by a quadratic. For convenience we may consider the related coefficients $c_3 = \alpha_3 - \alpha_5$, $c_4 = \alpha_3 + \alpha_5$, and $c_5 = \alpha_4$. Then we have $S = c_4$ and $C = \sqrt{{\alpha_3}^2 + {\alpha_5}^2}$.

In Eq. (1), if we continued to include subsequent high-order terms, they would take the form $\frac{1}{(m+n)!}s_{m,n}x^m y^n$, where $m+n$ is the order and

$$s_{m,n} = \frac{\partial^{m+n}}{\partial x^m \partial y^n} z(x,y). \tag{6}$$

These terms might also be converted into well-known representations. Zernike polynomials, for example, are a popular choice for describing high-order aberrations. Note that monomials of a given order can be directly converted to Zernikes of the same order with a linear transformation.[3] Recall that Zernike polynomials are popular due to the orthonormality over a unit disk. One might hope to exploit this orthonormality by generating a small patch of numbers describing a Zernike term centered at a point, and taking its product with the lens height map to compute the contribution of that term. However, here we have a sampled grid of points describing our surface at finite resolution, not a continuous disk, so orthonormality will not longer hold. However we can perform a broadly similar approach using specialized expansion terms.

The lens surface $z(x, y)$ will be described by an discrete grid $z(i, j)$ of dimension N by N, where i and j range from 1 to N. We seek the least-squares fit of a collection of monomials up to a chosen order with this discrete grid. Due to the uniform spacing of the grid, we can solve this problem for a single point (i_0, j_0) and apply the same solution with a translation to new points (i'_0, j'_0). So for gaze at a particular point (i_0, j_0), we seek the choices of $\alpha_{m,n}$ which minimize

$$\Omega(\alpha) = \sum_{i',j' \in A} \left(z(i' + i_0, j' + j_0) - \sum_{m,n} \alpha_{m,n} (i')^m (j')^n \right)^2 \tag{7}$$

over a small neighborhood of points described by the set R. We write this in terms of vectors and matrices as

$$\Omega(\boldsymbol{\alpha}) = \|\mathbf{z} - \mathbf{M}\boldsymbol{\alpha}\|_2^2, \tag{8}$$

where $\mathbf{z}$ is the surface points arranged into a vector of length N^2 (e.g., by concatenating columns), $\boldsymbol{\alpha}$ contains the unknown coefficients, and $\mathbf{M}$ is a matrix with columns given by vectors with elements $(i')^m (j')^n$ for all $i', j' \in R$. These columns have length l, the number of points in R. There are $p = \frac{1}{2}(m + n + 1)(m + n + 2)$ such columns (equal to the length of $\boldsymbol{\alpha}$). To avoid numerical issues, we choose a polynomial order $m + n$ such that $p < l$ and hence the least-squares solution to the above is $\boldsymbol{\alpha} = (\mathbf{M}^T\mathbf{M})^{-1}\mathbf{M}^T\mathbf{z} = \mathbf{P}\mathbf{z}$. Now with the rows of $\mathbf{P}$, we can directly estimate each of coefficients of components at a point.

However since we have $p < l$ this expansion will not completely describe the points in the region defined by R. We can generate the remaining components in a numerical stable way by computing the singular value decomposition

$$\mathbf{P} = \mathbf{U}\mathbf{S}\mathbf{V}^T. \tag{9}$$

This gives the nullspace of $\mathbf{P}$ as the bottom $l - p$ rows of $\mathbf{V}$, which we describe as $\mathbf{V}_N^T$. Then we form the combined matrix

$$\mathbf{Q} = \begin{pmatrix} \mathbf{P} \\ \mathbf{V}_N \end{pmatrix} \tag{10}$$

Which is of size $l \times l$ and nonsingular. The rows $\mathbf{q}_k$ of $\mathbf{Q}$ can be used to compute our complete discretized set of wavefront components plus nullspace components. Note that we only need to generate these terms once, as long as we use a similar neighborhood at every point on the lens. Then we reuse the rows $\mathbf{q}_k$ applied to the points in the neighborhood of every point on the lens to compute components.

An example is depicted in Fig. 2. Here the local neighborhood used is a circle of with diameter 7, which is nonzero for $l = 29$ points. The first four rows of terms in Fig. 2 contain the columns of $\mathbf{P}$, individually arranged into a small 2D images. These describe components of order 2,3,4, and 5, respectively. The last row contains the nullspace terms $\mathbf{V}_N$, describing the components of nonsmoothness that may remain after the 5^{th} order fit to the surface is computed. Fig. 3 gives an example of the coefficients computed using these high-order terms for a progressive lens design.

In Fig. 3 we can see a trend towards weaker values for increasing orders., which we'd expect for surface of high visual quality. At the extreme, nonsmoothness can cause scattering and difficulties in manufacture. So we'd want the highest order terms to be the smallest, particularly the nullspace terms. This is reflected in our analysis of real spectacle designs, where we see a trend as in Fig. 4.

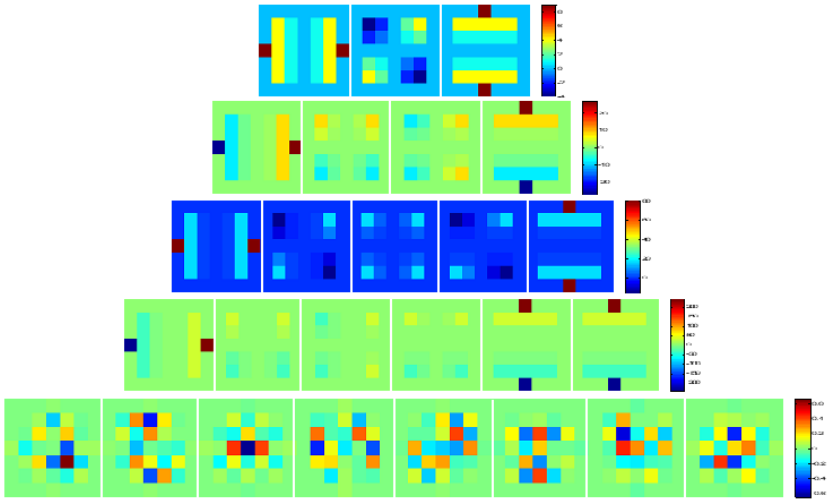

Figure 2. Second and higher-order terms used to compute expansion components in small region of lens.

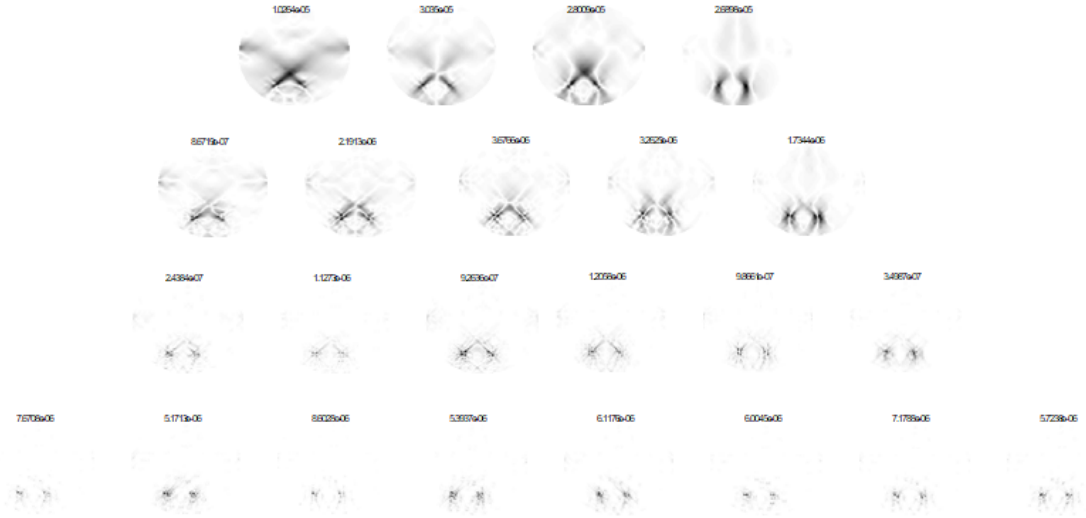

Figure 3. High order terms computed at each point in lens for a progressive lens design.

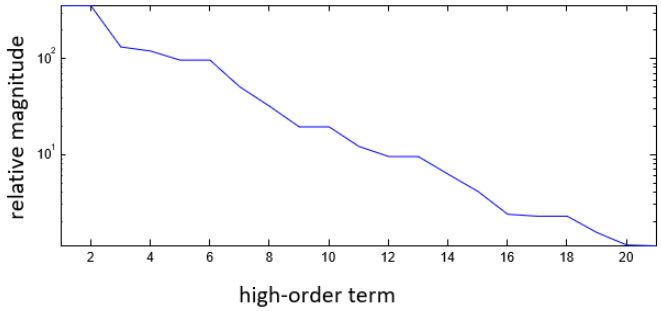

Figure 4. Variation with order for average magnitude of high-order components for real lenses.

2.1 Optimization Problem

For notational convenience, we define the matrix $\mathbf{A}_k$ to denote multiplication by the row $\mathbf{q}_k$ for each point on the lens. Then we form the optimization problem for minimizing the deviation from target values for each component at every point, here described as the vector $\mathbf{t}_k$. This minimization is also subject to constraints on particular

terms forming the quadratically-constrained quadratic program,

$$\begin{aligned} &\min_{\mathbf{z}} \textstyle\sum_{k=0}^{l} w_k \left\|\mathbf{A}_k\mathbf{z} - \mathbf{t}_k\right\|_2^2 \\ &\left\|(\mathbf{A}_k\mathbf{z} - \mathbf{t}_k)^{(r)}\right\|_2^2 \leq \mathbf{d}_k^{(r)},\ k = 0, ..., l,\ r = 0, ..., N^2, \end{aligned} \tag{11}$$

Here w_k is a relative weighting scalar we choose. The superscript r in the constraint refers to the r^{th} row of the vector. In effect, this is a set of constraints on each component in the wavefront expansion (indexed by k), for each point in the lens (indexed by r). The vectors $\mathbf{d}_k$ describe the maximum value allowed for the k^{th} component at each point.

To choose the targets and constraints for the low-order terms ($k = 3, 4, 5$), we can use the previously-described conversions between the monomials and a conventional sphere and cylinder representation. * We set the zeroth and first-order terms ($k = 0, 1, 2$) to control the final lens thickness and prism, for example with a simple constraint at lens center. For the high-order terms, ($k > 5$), we don't have any such intuitive idea of the desired constraints other than the overall trend of Fig. 4, though we generally will set their targets to zeroes. So for these terms we set increasing weights on the corresponding objective terms, and do not use constraints. In optimization problem (11) we constrain the 2^{nd} order components individually, but it may be useful (as well as efficient) to instead constraint the total power error with a constraint such as

$$\left\|(\mathbf{A}_3\mathbf{z} - \mathbf{t}_3)^{(r)}\right\|_2^2 + \left\|(\mathbf{A}_4\mathbf{z} - \mathbf{t}_4)^{(r)}\right\|_2^2 + \left\|(\mathbf{A}_5\mathbf{z} - \mathbf{t}_5)^{(r)}\right\|_2^2 \leq \mathbf{d}_{low}^{(r)}. \tag{12}$$

One could treat groups of higher-order terms for each order similarly to define a smooothness constraint.

2.2 Linearization

Of course, given the large range of refractive prescriptions, the visual performance of many spectacle lenses may be poorly-approximated by the above wavefront approach for low-order terms. The general nonlinear optimization problem would replace the matrices $\mathbf{A}_k$ with nonlinear functions $\mathbf{f}_k$ as in

$$\begin{aligned} &\min_{\mathbf{z}} \textstyle\sum_{k=0}^{l} w_k \left\|\mathbf{f}_k(\mathbf{z}) - \mathbf{t}_k\right\|_2^2 \\ &\left\|(\mathbf{f}_k(\mathbf{z}) - \mathbf{t}_k)^{(r)}\right\|_2^2 \leq \mathbf{d}_k^{(r)},\ k = 0, ..., l,\ r = 0, ..., N^2, \end{aligned} \tag{13}$$

where $\mathbf{f}_k(\mathbf{z})$ is a vector-valued function that computes the k^{th} component of the expansion at each point in the general (nonparaxial) case for the surface described by $\mathbf{z}$ in a lens system. For example, for $k = 3, 4, 5$, the function $\mathbf{f}_k(\mathbf{z})$ computes the true sphere and cylinder powers in a spectacle lens described by $\mathbf{z}$ when worn. All parameters describing the position of the eye and lens are built into this function. As we are only considering optimizing the back surface of a lens, the front surface is also assumed to be known parameters of the function as well as the refractive index.

We use ray-tracing to compute $\mathbf{f}_k(\mathbf{z})$. Ray tracing for spectacles is also relatively complex due to eye movement; we must determine the incoming ray direction for each gaze angle by first back-projecting rays outward from the eye, then determine the net lens power seen at the point by projecting a bundle or incoming rays in the reverse direction. We used the spectacle lens simulation tool SimuLens[4] which can simulate high resolution maps of lens sphere and astigmatism.

In general, given such a ray-tracing program, one could in theory use a standard optimization library to solve the problem (13), for example by using a gradient-free line-search method,[5] computing finite-difference derivatives, or using automatic differentiation.[6] However the large size of the problem coupled with the large number of inequality constraints presents a major challenge. Constrained optimization generally utilizes a second-order optimization method,[7] which requires memory usage on the order of the square of the number of variables

*This choice of indexing order for k is arbitrary, but see[3] for details on useful ways to relate the index k to the polynomial powers from m and n and order $m + n$, but generally it is helpful to index k to arrange terms in increasing polynomial order, which we assume here.

to describe the Hessian matrix. For a $N \times N$ lens, we have N^2 variables and hence memory scales as N^4. Further, optimizing this large size would be very slow as the complex ray-tracing function must be computed for all points over all expansion terms. As a result, most approaches to lens design describe the lens with a parametric representation such as a polynomial or spline surface using a number of parameters much smaller than N^2. This also allows them to sidestep the need to handle high-order terms as the parametric surface cannot describe nonsmooth surface. Of course it also may not be able to describe many completely valid surfaces that are more optimal.

Instead we will leverage the more efficient quadratic optimization program (11) as an inner solver, and use the ray-tracing program to compute iterative updates of the matrices $\mathbf{A}_k$ in a linearization step. The Jacobian of $\mathbf{f}_k$ is a matrix with elements describing the derivative of lens point z_r with respect to lens point z'_r.

$$J_{r,r'} = \frac{\partial \mathbf{f}_k^{(r)}(\mathbf{z})}{\partial z'_r} \tag{14}$$

Since we have assumed that points outside a small neighborhood do not affect visual performance at a given point, we only need to compute a small number of terms for each row of the Jacobian. However, the gradient of a raytracing calculation on a high-resolution surface with respect to perturbations at individual nearby points may also cause difficulties, depending on the method. So we would like to constrain the gradient updates to only consider optically smooth changes to the surface. If we write the raytracing function for a particular term and point as

$$\mathbf{f}_k(\mathbf{z}_0 + \Delta) = \mathbf{f}_k\left(\mathbf{z}_0 + \sum_{r'=1}^{l} \delta_{r'} \mathbf{e}_{r'}\right) \tag{15}$$

where z_0 is a constant, $\delta_{r'}$ are the elements of the surface adjustment variable Δ, and $\mathbf{e}_{r'}$ are vectors with a single nonzero value at point r' with unit magnitude. The derivatives of Eq. (14) are then equivalently the derivates with respect to $\delta_{r'}$. So we can represent this using our complete set of polynomial terms $\{q_k\}$ as

$$\mathbf{f}_k(\mathbf{z}_0 + \Delta) = \mathbf{f}_k\left(\mathbf{z}_0 + \sum_{r'=1}^{l} \hat{\delta}_{r'} \mathbf{q}_{r'}\right) \tag{16}$$

where $\delta_{r'}$ and $\delta_{r'}$ are related by linear transformation, and the Jacobian is computed with respect to $\hat{\delta}_{r'}$. Now we can enforce smoothness of the gradient by limiting the terms used above, e.g. to exclude the nullspace terms or perhaps a lower cutoff in high order, depending on the ray-tracing algorithm's capabilities and speed.

While we may discard some components in the above linearization step, we do not ignore them in the optimization; we simply continue to use the paraxial versions instead. This fits the problem well since the largest terms (most requiring of linearization updates) are the lowest orders and therefore smoothest, while the highest-order terms are the smallest and for which paraxial approximation works best. Therefore our final optimization problem is again a QCQP similar to Eq. (11), but with periodically updated matrices $\mathbf{A}'_k$ for the lower orders. For these terms we to replace the q_k term in each column with a sum over gradient elements of the form

$$q'_k = \sum_{r'=1}^{l} \frac{\partial}{\partial \delta_{r'}} \mathbf{f}_k\left(\mathbf{z}_0 + \hat{\delta}_{r'} \mathbf{q}_{r'}\right) q_{r'}. \tag{17}$$

At subsequent updates, we must also adjust the nonzero targets to each new linearization point.

3. RESULTS

Here we provide an example of the use of this method for optimizing progressive addition lenses for presbyopia. Such lenses attempt to provide a so-called far zone in the upper region of the lens for distance vieweding, and a near zone in the lower region of the lens for reading.[8] Unlike bifocal lenses which also provide these zones, progressives attempt to provide a smooth and usable transition between far and near for intermediate distance

viewing, known as the channel. Also a number of other trade-offs must be considered to optimize both wearer comfort and performance.[9] As a result, it is useful to be able to design a variety of different lens styles.

To use the proposed approach, we choose targets $\mathbf{t}_k$ which give the prescription, and constraints $\mathbf{d}_k$ which give the maximum allowed deviations from target powers at every point. Fig. 5 demonstrates the design process for an example. Fig. 5(a) describes the structure we plan to use, with widths at various heights that we constraint to higher optical quality. Figs. 5(b) and (c) give simulations of the resulting optimized sphere and cylinder powers, respectively.

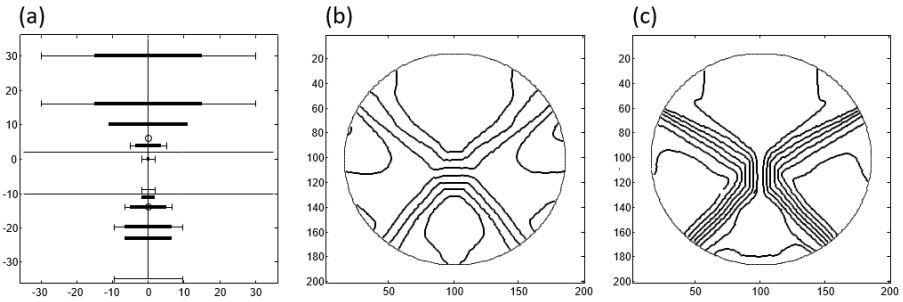

Figure 5. Designed constraint shapes (a), and resulting sphere (b) and cylinder (c) contour plots for optimized surface. The contours are spaced at 0.25 D increments.

With this approach, we can easily change the design as desired by changing the constraint ranges. For example, by shifting the lower reading area to more nasal to allow convergence of eyes as in Fig. 6 or by changing the length of the channel to fit different frames as in Fig. 7.

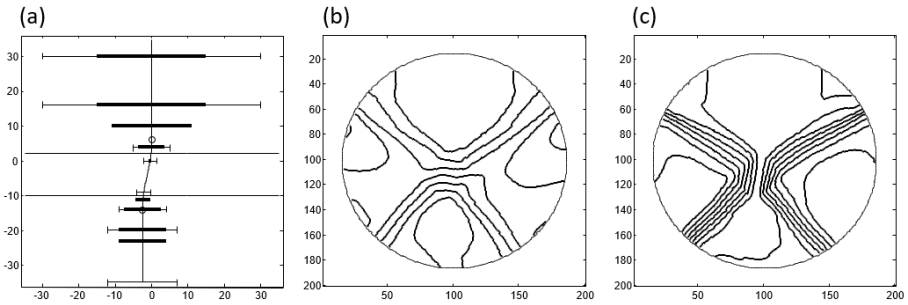

Figure 6. Designed constraint shapes (a), and resulting sphere (b) and cylinder (c) contour plots for optimized surface with inset. The contours are spaced at 0.25 D increments.

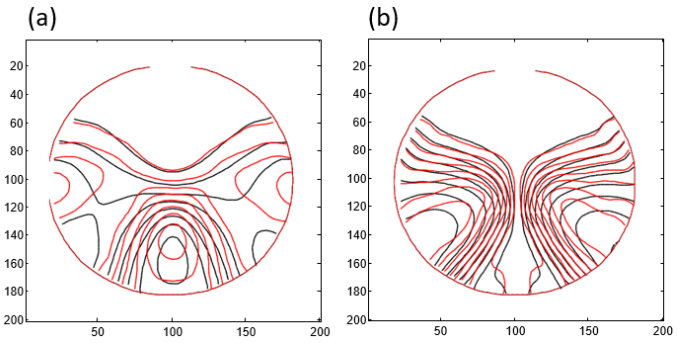

Figure 7. Contour plots of sphere (a) and cylinder (b) for optimized surface with long (black) and short (red) channel design. The contours are spaced at 0.25 D increments.

4. CONCLUSION

We considered the nonparametric optimization of high-resolution spectacle lens surfaces. By expanding the components of local descriptions of the surface into low and high order components, we could address both the large powers and nonsmoothness within the same formulation. As our design process involved simply stipulating the desired powers and ranges, it is easy to adapt to various other lenses. Examples include lenses for myopia control[10] and smooth bifocals. Spectacle design has primarily been focused on low order components and parametric surface descriptions, so there is only limited domain knowledge in the literature regarding what are useful features of high-order components (apart from simply trying to eliminate them). However there has been some investigation in high-order components enabled by recent wavefront sensing tecnhologies.[11,12] The approach presented here could allow for an even more powerful control of the lens design, if more information on the high-order requirement were known. This could also be useful in myopia control where such components may play an important role.[13]

REFERENCES

[1] Jalie, M., "Modern spectacle lens design," *Clinical and Experimental Optometry* **103**, 3–10 (Jan. 2020). Publisher: Taylor & Francis _eprint: https://doi.org/10.1111/cxo.12930.

[2] Campbell, S. D. and Jungwirth, M. E. L., "Special Section Guest Editorial: Advances in Computational Methods for Optical System Forward- and Inverse-Design," *Optical Engineering* **62**, 021001 (Feb. 2023). Publisher: SPIE.

[3] Dillon, K., "Bilinear wavefront transformation," *Journal of the Optical Society of America A* **26**(8), 1839–1846 (2009).

[4] FormuLens, "SimuLens Functionality," *http://www.formulens.com/notebooks/SimuLensDemo01.html* (2020).

[5] Gill, P. E., Murray, W., and Wright, M. H., [*Practical Optimization*], SIAM (Dec. 2019).

[6] Sun, Q., Wang, C., Fu, Q., Dun, X., and Heidrich, W., "End-to-end complex lens design with differentiate ray tracing," *ACM Transactions on Graphics* **40**, 71:1–71:13 (July 2021).

[7] Battiti, R., "First- and Second-Order Methods for Learning: Between Steepest Descent and Newton's Method," *Neural Computation* **4**, 141–166 (Mar. 1992).

[8] Meister, D. J. and Fisher, S. W., "Progress in the spectacle correction of presbyopia. Part 1: Design and development of progressive lenses," *Clinical and Experimental Optometry* **91**, 240–250 (May 2008). Publisher: Taylor & Francis _eprint: https://doi.org/10.1111/j.1444-0938.2007.00245.x.

[9] Sheedy, J. E., "Progressive addition lenses—matching the specific lens to patient needs," *Optometry - Journal of the American Optometric Association* **75**, 83–102 (Feb. 2004).

[10] Sankaridurg, P., Donovan, L., Varnas, S., Ho, A., Chen, X., Martinez, A., Fisher, S., Lin, Z., Smith, E. L., Ge, J., and Holden, B., "Spectacle lenses designed to reduce progression of myopia: 12-month results," *Optometry and Vision Science: Official Publication of the American Academy of Optometry* **87**, 631–641 (Sept. 2010).

[11] Chamadoira, S., Sasian, J., and Acosta, E., "Interferometric Local Measurements of High-Order Aberrations in Progressive Addition Lenses," *Optometry and Vision Science* **92**, 1047 (Nov. 2015).

[12] Villegas, E. A. and Artal, P., "Comparison of aberrations in different types of progressive power lenses," *Ophthalmic and Physiological Optics* **24**(5), 419–426 (2004). _eprint: https://onlinelibrary.wiley.com/doi/pdf/10.1111/j.1475-1313.2004.00214.x.

[13] Hughes, R. P., Vincent, S. J., Read, S. A., and Collins, M. J., "Higher order aberrations, refractive error development and myopia control: a review," *Clinical and Experimental Optometry* **103**, 68–85 (Jan. 2020). Publisher: Taylor & Francis _eprint: https://doi.org/10.1111/cxo.12960.